PHYSICAL REVIEW B VOLUME 15, NUMBER 2 15 JANUARY 1977

Structure, bonding, and stability of topologically close-packed intermetallic compounds

J. Hafner
Max-Planck-Institut für Festkörperforschung, D 7 Stuttgart, Federal Republic of Germany
(Received 31 August 1976)

An orthogonalized-plane-wave-based first-principles pseudopotential method is presented for calculating the crystal structure, lattice constants, enthalpy, and volume of formation of binary intermetallic compounds and alloys. The pseudopotential is optimized specifically for the case of binary systems. The $X\alpha$ method is used to construct the electron-ion potential. The theory is applied to investigate the random binary alloys and ordered intermetallic compounds between alkali metals. The crystal structure of the intermetallic phases (Na_2K, Na_2Cs, K_2Cs, and K_7Cs_6) which belong to the type of topologically close-packed (Frank-Kasper) phases is successfully explained in terms of a delicate balance between electrostatic and band-structure forces. The enthalpies and volumes of formation and the range of stability of these phases are calculated with good accuracy—with the exception of Na_2Cs, however. It is argued that *s-d* hybridization is vital for the formation of Na_2Cs. The physical principle governing the bonding is shown to be close-packing, described in terms of soft interionic potentials.

I. INTRODUCTION

It has been pointed out by Frank and Kasper,[1] that a large number of the relatively complex structures of intermetallic compounds may be considered as determined by the geometrical requirements of sphere packing. Though the topological and geometrical properties of these crystal lattices are thoroughly understood, a microscopic understanding of their structure and their bonding properties in terms of the electronic band structure is still lacking.

Most of these compounds are formed by transition metals. Very recent investigations of Simon and co-workers[2,3] renewed the interest in close-packed intermetallic compounds formed by nontransition metals. In their search for intermetallic phases in the binary alkali-metal systems they showed that, besides the well-established hexagonal Laves phase ($C14$ in the Strukturbericht[4] notation) Na_2K,[5] there exist two isostructural phases with composition Na_2Cs (previously investigated by Rinck[6] and Goria[7]) and K_2Cs, whereas an occasionally postulated compound Na_2Rb definitely does not exist. Moreover, they discovered the existence of a compound K_7Cs_6 whose crystal structure is a stacking variant of the well-known μ phase in binary transition-metal systems ($D8_5$, examples Fe_7W_6 and Co_7Mo_6). Because of the free-electron-like character of the electronic structure of their constituents, these phases represent the simplest possible application for any electronic theory of their bonding properties.

We present here an *ab-initio* treatment of the binary alkali-metal intermetallic phases in terms of the optimized first-principles theory originally developed by Harrison[8] and recently generalized to binary systems by the present author[9] (hereafter, this paper will be referred to as I). The pseudopotential is optimized in the sense that the pseudo-wave-function is smooth and that the perturbation expansion has optimal convergence properties. This is particularly important for highly complex structures and for disordered alloys, because in these cases small wave numbers (and correspondingly large pseudopotential matrix elements) contribute to the total energy. The theory takes full account of the change on alloying of the pseudopotential of the components due to the change in the chemical potential, the change in the crystal potential, the change in the core shifts and due to the presence of a second kind of core states. It has been successfully applied to calculate the structural, thermochemical and thermomechanical properties of solid Li-Mg alloys[9] and of some liquid alloys.[10]

In the present work, it is applied to calculate the enthalpy of formation of binary alkali-metal compounds with stoichiometry AB_2, A_6B_7, and A_4B_3 with the possible crystal structures classified by Frank and Kasper.[1] In addition, we calculate the enthalpy of formation of the concurring solid solutions. To gain more insight into the bonding mechanism, the positional parameters describing the distribution of the atoms within the elementary cell are varied. It turns out that the observed structures do not correspond to a minimum in the electrostatic (Ewald) energy of the ions, but may be described in terms of a balance of electrostatic and electronic band-structure contributions. In this context it is very instructive to examine the effective interatomic potentials describing the forces between A-A, A-B, and B-B pairs of atoms. Possible contributions of

(s-d) hybridization to the stabilization of the Na_2Cs phase will be shortly discussed.

II. OPTIMIZED PSEUDOPOTENTIAL IN BINARY SYSTEMS

The optimized first-principles pseudopotential theory has been developed in full detail in I, so it will be sufficient to stress the main lines here. As for pure metals our starting point is the one-particle Schrödinger equation

$$H|\psi\rangle = (T+U)|\psi\rangle = E|\psi\rangle\,, \tag{1}$$

with the self-consistent crystal potential U which is a linear superposition of individual ionic contributions U_A, U_B from both kinds of ions. Expanding the eigenstates of the Hamiltonian (1) in terms of generalized orthogonalized plane waves[11]

$$|\chi\rangle_{\vec{k}} = |\vec{k}\rangle - \sum_{j(A)} \sum_{t} |\vec{r}_j, At\rangle \langle \vec{r}_j, At|\vec{k}\rangle - \sum_{j(B)} \sum_{s} |\vec{r}_j, Bs\rangle \langle \vec{r}_j, Bs|\vec{k}\rangle\,. \tag{2}$$

[$|\vec{k}\rangle$ stands for a plane wave and $\langle \vec{r}|\vec{r}_j, At\rangle = \psi_t^A(\vec{r}-\vec{r}_j)$ for core states of type A, centered at $\vec{r}_j$ and labeled by the set of quantum numbers t], we obtain a Phillips-Kleinman[12] equation for a binary system. The pseudopotential is then optimized by applying the criterion of the smoothest possible wave function as formulated by Cohen and Heine.[13] After a lengthy calculation (for any details, cf. I) we arrive at the following factorized form of the pseudopotential matrix element

$$\langle \vec{k}+\vec{q}|W|\vec{k}\rangle = S_A(\vec{q})\langle \vec{k}+\vec{q}|w_A|\vec{k}\rangle + S_B(\vec{q})\langle \vec{k}+\vec{q}|w_B|\vec{k}\rangle\,. \tag{3}$$

S_A and S_B are the partial structure factors describing the spatial arrangement of A and B ions, respectively,

$$\begin{aligned} S_A(\vec{q}) &= N^{-1} \sum_{j(A)} \exp(-i\vec{q}\cdot\vec{r}_j), \\ S_A(0) &= N_A/N \equiv (1-c), \\ S_B(\vec{q}) &= N^{-1} \sum_{j(B)} \exp(-i\vec{q}\cdot\vec{r}_j), \\ S_B(0) &= N_B/N \equiv c\,. \end{aligned} \tag{4}$$

N_A, N_B, $N = N_A + N_B$ stand for the numbers of ions, c is the concentration of the B component. The form factors for the component A are given by

$$\langle \vec{k}+\vec{q}|w_A|\vec{k}\rangle = u_A(q) + \sum_t (k^2 + \langle \vec{k}|W|\vec{k}\rangle - E_t^A) \times \langle \vec{k}+\vec{q}|0,At\rangle\langle 0,At|\vec{k}\rangle \tag{5}$$

with the diagonal element

$$\langle \vec{k}|W|\vec{k}\rangle = (1-c)\langle \vec{k}|w_A|\vec{k}\rangle + c\langle \vec{k}|w_B|\vec{k}\rangle\,, \tag{6}$$

$$\langle \vec{k}|w_A|\vec{k}\rangle = u_A(0) + (1-\langle \vec{k}|P|\vec{k}\rangle)^{-1} \times \sum_t (k^2 + \overline{U} - E_t^A)|\langle 0,At|\vec{k}\rangle|^2\,, \tag{7}$$

with

$$\overline{U} = (1-c)u_A(0) + cu_B(0)\,, \tag{8}$$

and the projection operator matrix-elements

$$\langle \vec{k}|P|\vec{k}\rangle = (1-c)\sum_t |\langle 0,At|\vec{k}\rangle|^2 + c\sum_s |\langle 0,Bs|\vec{k}\rangle|^2\,. \tag{9}$$

The corresponding equations hold for the B component with u_A, E_c^A, and $\langle 0,At|$ replaced by u_B, and E_B, $\langle 0,Bs|$, respectively.

In practice, the self-consistent crystal potential U is not known. We have to start with the bare electron-ion potentials U_A^0, U_B^0, construct a bare pseudopotential W^0 by using them in Eqs. (5)–(9). This bare pseudopotential is then made self-consistent by linearily screening it by a homogeneous electron gas of the density $\rho = \overline{Z}/\Omega$. $\overline{Z}$ is the average valence. Ω is the volume per atom (we do not assume a linear variation of Ω with concentration, but rather determine the atomic volume for each concentration and each phase from the thermodynamic stability criterion, see below). Exchange and correlation among the valence-electrons are treated in the Vashishta-Singwi[14] approximation.

The construction of the electron-ion potentials, based on the $X\alpha$ method, and the calculation of the core shift appropriate for alloys have been described in previous papers,[9, 15, 16] only the following points should be made: (a) the only disposable parameter in the potential describes the many-body interactions between core and valence electrons. It has been demonstrated that its introduction at this stage is natural as well as necessary and that it allows one to account for the nonlinearity of the pseudopotential in the valence charge density in a simple way and to give an accurate description of a wide range of different properties of the pure metals. No new parameter is introduced for the binary phases. (b) From the discussion it is immediately evident that the form factor of both components in the alloys is different from that of the pure metals due to (i) the change in the Fermi level, (ii) the change in the average crystal potential $\overline{U}$, (iii) the change in the core shift, and finally (iv) due to the presence of a second kind of core states in the projection operator P [Eq. (9)]. This last point is also important in determining appropriate effective val-

encies (defined as the nominal valence plus the charge of the orthogonalozation hole) Z_A^*, Z_B^* for the ions in the alloy [cf. Eq. (25) of I].

III. TOTAL ENERGY AND INTERATOMIC POTENTIALS

The calculation of the total energy of a binary system is somewhat lengthy, but in principle straightforward. As a result, we obtain three different contributions (i) the structure-independent free-electron energy $E_{\rm fe}$ [Eq. (33) of I], (ii) the electrostatic energy of point ions with effective valencies Z_A^* and Z_B^* in a negative compensating background. For the case of an ordered compound it is given by

$$E_{\rm es} = (Z_A^* \alpha_{AA} + Z_A^* Z_B^* \alpha_{AB} + Z_B^{*2} \alpha_{BB})/r. \tag{10}$$

Here r is the radius of an average atomic sphere $r = (3\Omega/4\pi)^{1/3}$, and the α's are the geometrical Ewald coefficients of the lattice which may be calculated using the well-known Ewald-Fuchs method.[17] For a disordered alloy, the electrostatic energy is given by[18]

$$E_{\rm es} = Z^{*2}\alpha/r, \quad Z^* = (1-c)Z_A^* + c\,Z_B^*\,, \tag{11}$$

α being the Ewald parameter of the underlying perfect lattice. The last contribution is (iii) the band-structure energy $E_{\rm bs}$ given by

$$E_{\rm bs} = \sum_{i,j} \sum_{\vec{q}}{}' S_i^*(\vec{q}) S_j^*(\vec{q}) F^{ij}(\vec{q})\,. \tag{12}$$

Here there are two alternative formulations:
(i) S_i, S_j are the partial structure factors defined above, the energy wave number characteristics F^{ij} are given by

$$F^{ij}(q) = \frac{2\Omega}{(2\pi)^3} \int_{|\vec{k}| \le k_F} \frac{\langle \vec{k}+\vec{q}|w_i|\vec{k}\rangle \langle \vec{k}|w_j|\vec{k}+\vec{q}\rangle}{K^2 - |\vec{k}+\vec{q}|^2}\, d^3k - \frac{q^2}{16\pi} \frac{w_i^{\rm scr}(q) w_j^{\rm scr}(q)}{1-G(q)}\,, \tag{13}$$

with $i,j = A,B$, the w_i, $w_i^{\rm scr}$ standing for the form factors w_A, w_B and the corresponding screening potentials.
(ii) S_i, S_j stand for the structure factors S and D

$$S = S_A + S_B\,, \qquad D = cS_A - (1-c)S_B\,, \tag{14}$$

defined by Hayes *et al.*,[19] and w_i and $w_i^{\rm scr}$ in Eq. (18) are to be replaced by the corresponding average and difference terms, cf. I. Since $D^*S = DS^* = 0$, $D(0) = 0$, and D^*D = constant for random alloys with lattices in which all sites are equivalent,[20] this formulation is most convenient for solid solutions.

The energy wave-number characteristics F^{AA}, F^{AB}, F^{BB} describe an indirect ion-electron-ion interaction in wave-number space between A-A, A-B, and B-B ions. Fourier transforming and adding the direct Coulomb repulsion between the point ions, we obtain effective pair potentials for the interionic forces in the alloy.[10] Again, it is to be emphasized that the interaction between two ions will be different in the pure metal and in the alloy.

IV. ENTHALPY AND VOLUME OF FORMATION

We have now collected all necessary ingredients for the calculation of the total energy, the zero-pressure lattice constant, and the isothermal bulk modulus for body-centered solid solutions and for intermetallic compounds with different crystal structures. Similar calculations for the pure alkali metals have been reported.[16] At a given temperature and pressure, the stable phase is the one with the lowest free enthalpy $G = E + p\Omega - TS$. Restricting ourselves to $T = 0$ °K, the entropy S vanishes and it is sufficient to calculate the enthalpy $H = E + p\Omega$. At zero pressure, the enthalpy of formation is then given by

$$\Delta H(c) = E_{AB}(c, \Omega_{AB}) - (1-c)E_A(\Omega_A) - cE_B(\Omega_B), \tag{15}$$

where Ω_{AB}, Ω_A, Ω_B are the zero-pressure atomic volumes of the A-B alloy and of the pure metals, respectively. The excess volume for the formation of the alloy is given by

$$\Delta\Omega = \Omega_{AB} - (1-c)\Omega_A - c\Omega_B\,. \tag{16}$$

V. SOLID SOLUTIONS

At sufficiently low temperature, Li is immiscible with all other alkali metals. Na is immiscible with the heavier alkalis in the solid state, but forms a continuous sequence of liquid solutions. K-Rb, K-Cs, and Rb-Cs form solutions both in the liquid and in the solid state, but in the K-Cs system the intermetallic phases K_2Cs and K_7Cs_6 are stable below −90 °C.[2,3] The calculated enthalpies display the behavior expected from Hume-Rothery's 15% rule (Fig. 1). For the K-Rb, K-Cs, and Rb-Cs systems, the positive sign and magnitude is in reasonably good agreement with the ΔH estimated by Yokokawa and Kleppa[22] from liquid-metal data, K-Rb: $\Delta H = 156(46)$ cal/g atom, K-Cs: $\Delta H = 800$ (166) cal/g atom, Rb-Cs: $\Delta H = 120(13)$ cal/g atom. ΔH is somewhat overestimated because the differences in the theoretical densities are somewhat greater than the corresponding experimental differences (cf. Ref. 16 for a complete theoretical description of a wide range of properties of the pure alkali metals). Figure 2(a) re-

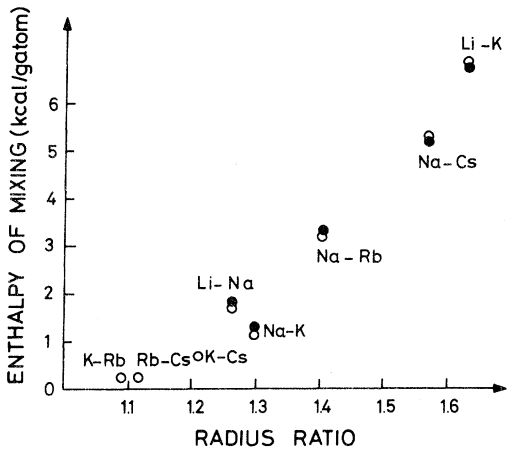

FIG. 1. Enthalpy of mixing for body-centered cubic alkali-metal solid solutions against the ratio of the atomic radii of the pure components. Full dots for the equiatomic composition, the open circles stand for a concentration of 67 at.% of the lighter component.

presents the variation of the lattice constants with concentration. Large positive enthalpies of mixing are correlated with positive deviations of the lattice constant from the linear relation, whereas for systems with small ΔH, the lattice constant varies strictly linear, in agreement with experiment.[3, 25] In terms of the excess volume of alloying, our calculations yield: $\Delta\Omega/\Omega = 1.77\%$ (Li-Na), -1.47% (LiK), -0.34% (NaK), $+0.32\%$ (NaRb), $+0.59\%$ (NaCs), -0.12% (KRb), $+0.51\%$ (KCs), and -0.17% (RbCs), respectively. Hence there is no appreciable change of volume on alloying. Figure 2(b) represents the variation of the isothermal bulk modulus B_T with concentration. Large negative deviations from linearity are observed for the hypothetical (immiscible) binary phases. For the existing solid solutions, B_T varies nearly linearly. No experimental high-pressure investigations of alkali-metal solid solutions are known. In summary, our calculation predicts an ideal solution behavior for the solid alloys of K-Rb, Rb-Cs and, to slightly lesser extent, K-Cs.

VI. LAVES PHASES

The crystal structures based on the close packing of equal spheres may be regarded as assembled by triangular layers which are the closest packing in two dimensions. There is a double choice in stacking each layer on the next. They may be designated as ∇ and Δ and any repeating sequence defines a member of an infinite series of close-packed structures, of which the face-centered cubic and the hexagonal close-packed

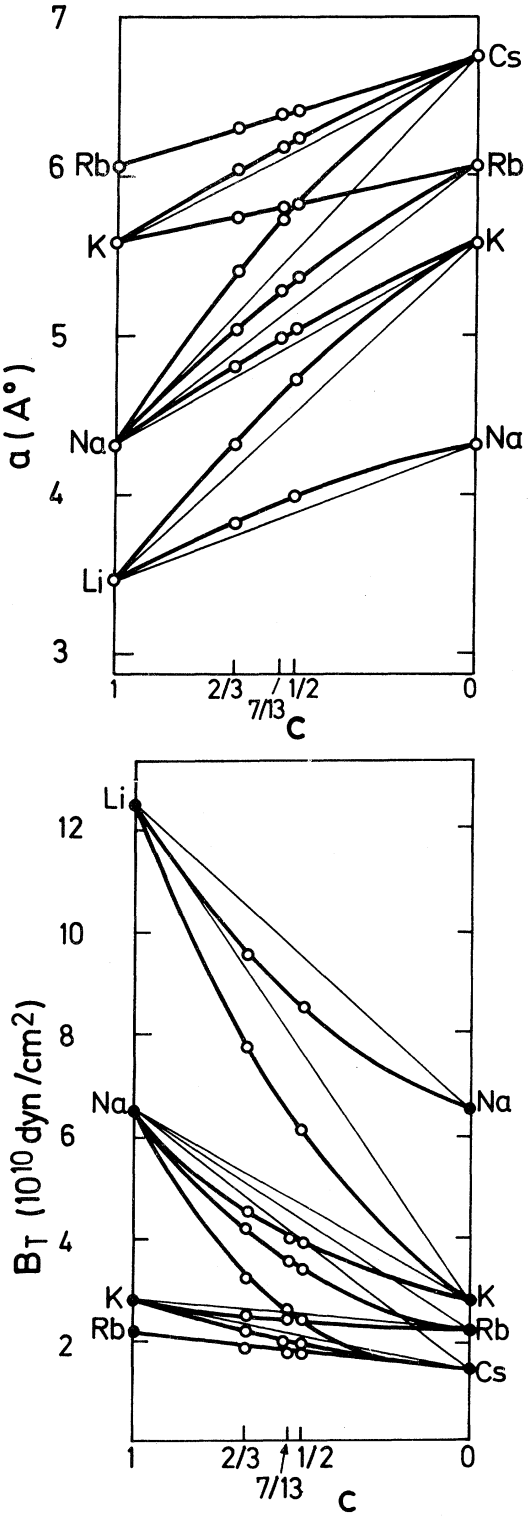

FIG. 2. Lattice constant (a) and isothermal bulk modulus (b) of body-centered cubic solid solutions of the alkali metals. The open circles indicate the calculated results, the bold lines are drawn to guide the eyes. The thin lines connect the pure metal values.

lattices are the simplest examples.

In analogy to this the close-packed intermetallic compounds may be considered as different stacking sequences of one or more different sandwiches of layers.[1] For the Laves phases AB_2 such a sandwich is made up of a Kagomé net of B atoms, a triangular net of A atoms centering its hexagons, then a triangular net of B-atoms centering half of the Kagomé triangles (e.g., those in orientation Δ), and by a third triangular net of A atoms centering the remaining triangles. A second Kagomé-layer of B atoms, with its ∇ triangles over the Δ triangles of the first one begins the next sandwich, which may be similar to the first one, or alternatively have its triangular B net over the ∇ triangles of the Kagomé net. The first stacking is called Δ, the second ∇, and an infinite series of structures is described by the different sequences of Δ and ∇.

Repeated Δ stackings make the cubic Laves phase $C15$ ($MgCu_2$-type). The repeated sequence $\Delta\nabla$ makes the hexagonal Laves phase $C14$, typified by $MgZn_2$. The sequence $\Delta\Delta\nabla\nabla$ defines the Laves phase $C36$ ($MgNi_2$ type). The crystallographic description of the three Laves phases is summarized in Table I, the positional parameters are given for the ideal structure. For the ideal structure, the larger A atoms form a diamond sublattice for $C15$ and a wurtzite-like sublattice for $C14$, the sublattice in $C36$ being a mixture of the two structures. In all three phases, the smaller B atoms form different tetrahedral networks.[24] The lattices are compared in Fig. 3 in form of a projection on the (110) plane. In this representation, the structure may be regarded as a sequence of planar networks, so-called primary nets in which the atoms form pentagons and triangles (emphasized in Fig. 3 by continuous lines connecting the atoms) alternate with secondary nets with triangular arrangement (the black circles in Fig. 3).

The larger A atoms are surrounded by four other A atoms and 12 B, while the B atoms have 6 A and 6 B as nearest-neighbors. Compared at constant atomic volume, the nearest-neighbor distances d_{AA}, d_{AB}, and d_{BB} are identical for all three structures.

A. Structural energy differences

First, we considered the ideal structures. It turns out that the hexagonal $C14$ lattice is always energetically more favorable (Table II)— in agreement with the observed crystal structures. If we examine the electrostatic and electronic contributions separately, we find that the electrostatic energy prefers a cubic arrangement of the ions (Table I). For both the A and B sublattices, the

TABLE I. Crystallographic description and Ewald coefficients for the Laves phases. The structural parameters are given for the ideal structures. The notation is that of the International Tables for X-Ray Crystallography, Ref. 23. The Ewald coefficients are given also for the parameters minimizing the electrostatic energy for $Z_A = Z_B$. $\alpha = \alpha_{AA} + \alpha_{AB} + \alpha_{BB}$.

$C15$—$MgCu_2$ type		Space group $Fd3m - O_h^7$		
Atomic positions:				
8 A atoms in (a); 16 B atoms in (d).				
Ewald coefficients:	α_{AA}	α_{AB}	α_{BB}	α
	−0.386 168	−0.478 229	−0.907 916	−1.772 313
$C14$—$MgZn_2$ type		Space group $P6_3/mmc - D_{6h}^4$		
Atomic positions:				
4 A atoms in (f), $z = \frac{1}{16}$;				
2 B atoms in (a); 6 B in (h), $x = -\frac{1}{6}$.				
Axial ratio: $c/a = (\frac{8}{3})^{1/2} = 1.633$				
Ewald coefficients:	α_{AA}	α_{AB}	α_{BB}	α
Ideal structure	−0.385 602	−0.480 707	−0.905 207	−1.771 515
$z = 0.070$				
$z = -0.180$	−0.383 662	−0.473 688	−0.917 111	−1.774 461
$c/a = 1.52$				
$C36$—$MgNi_2$ type		Space group $P6_3/mmc - D_{6h}^4$		
Atomic positions:				
4 A atoms in (e), $z = \frac{3}{32}$; 4 A in (f), $z = \frac{27}{32}$;				
6 B atoms in (g); 6 B in (h), $x = \frac{1}{6}$; 4 B in (f), $z = \frac{1}{8}$.				
Axial ratio: $c/a = 2(\frac{8}{3})^{1/2} = 3.266$				
Ewald coefficients:	α_{AA}	α_{AB}	α_{BB}	α
Ideal structure	−0.385 892	−0.479 431	−0.906 597	−1.771 920
$c/a = 3.24$				

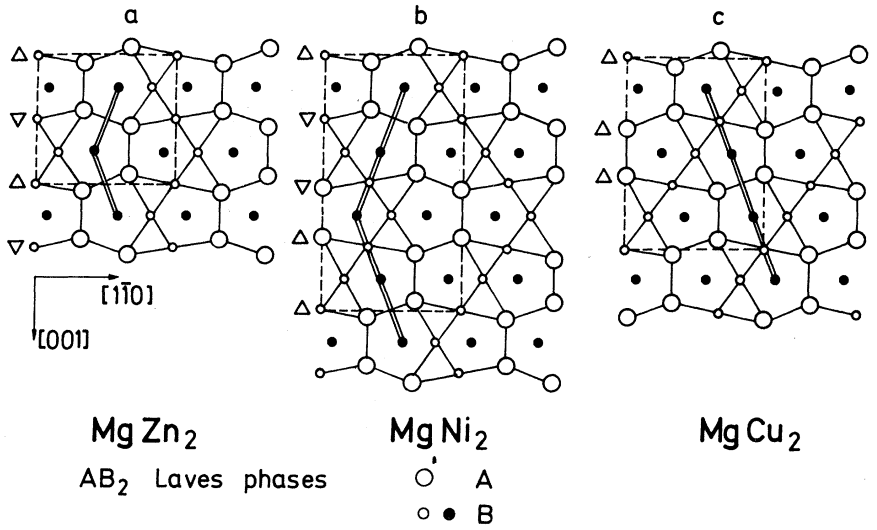

FIG. 3. Comparison of the three Laves-phase structures in form of a projection on the (110) plane. The primary networks are emphasized by the lines connecting the atoms. For sake of clarity the second primary network (antisymmetric to the first one) has been omitted. The secondary network is built by the majority atoms represented by full dots. These atoms lie in the Kagomé planes. The double lines connect equivalent positions in the Kagomé planes to emphasize the stacking sequence.

Ewald energy is lower for the $C15$ than for the $C36$ and $C14$ structure.

The A sublattice of $C15$ is of diamond type ($A4$), hence the coefficient $\alpha_{AA}(C15)$ should be directly related to the Ewald constant of the diamond lattice. Taking the change in the number of atoms per unit cell and the change in the mean atomic radius into account, we have $3\times 3^{1/3}\alpha_{AA}(C15) = 1.670\,852 = \alpha(A4)$, in excellent agreement with previously published values.[8,26] Similar cross checks are possible for the other structures. This is important, since the two Ewald constants for the $MgZn_2$ lattice reported by other authors[27,28] are definitely in error. On the other side, good agreement is observed between our calculations and unpublished results of Hoppe.[29] The A-B coordination is electrostatically more favorable in the hexagonal stacking variants, but as a whole, the Ewald energy is lowest for the cubic $C15$ lattice.

The band-structure contribution to the total energy is given by Eq. (12). In Fig. 4 we have plotted the energy wave number characteristics, conveniently normalized to unity for $q=0$, together with the corresponding structural weight function N (defined as the square of the structure factor times the multiplicity of the reciprocal lattice vector) for the compounds Na_2K and K_2Cs. The lowering of the symmetry in the hexagonal Laves phases is reflected by the distribution of the structural weight over a larger number of reciprocal lattice vectors. For the A-A and B-B in-

TABLE II. Equilibrium lattice constant, enthalpy, and volume of formation of the $C14$ Laves phases (assuming the ideal structural parameters) and structural energy differences of the $C15$ and $C36$ phases relative to the $C14$ phase.

	a (Å)		ΔH (cal/g atom)			ΔE (cal/g atom)	
	Theory	Experiment	Theory	Experiment	$\Delta\Omega/\Omega$(%)	$C15$	$C36$
Li_2Na	3.95		680		0.1	119	62
Li_2K	4.73		3600		−7.5	187	156
Na_2K (id)	7.74	7.50[a]	−63	−145[b]	−1.5	94	63
(min)	7.62		−125		−1.5		
Na_2Rb	8.01		1100		−5.4	125	93
Na_2Cs	8.38	7.86[d]	2070		−11.6	156	125
K_2Rb	9.38		30		3.0	63	63
K_2Cs (id)	9.69	9.07[c]	−125		−1.3	125	84
(min)	9.56		−180		−1.3		
Rb_2Cs	10.24		−130		0.6	94	63

[a] Reference 5, room temperature.
[b] Reference 21, $T=280$ °K.
[c] Reference 2, $T=178$ °K.
[d] Reference 2, $T=223$ °K.

teractions, this results in energetically more favorable contributions from short reciprocal lattice vectors for the $C14$ than for the $C15$ structure. For the A-B interactions, the structural weight is positive only in that region where the characteristic F_N^{AB} is very small or even negative. This means that the indirect ion electron-ion interactions between unlike ions are energetically quite unfavorable for all three Laves phases. Here again, the structure of the $C14$ phase is better adapted to the particular form of the characteristic.

In Fig. 4(a) we have included the characteristics of K-K ion interactions both in the Na_2K and in the K_2Cs phases. They are seen to be drastically different. This illustrates the strong dependence of the pseudopotential and hence of the indirect ion-electron-ion interactions of one of the components on the second component and its concentration, as has been emphasized in Sec. II.

B. Crystal structure of the $C14$ phases

To obtain a better insight into the physical mechanism governing the particular arrangement of ions in such topologically close-packed phases, we have calculated the binding energy of the hexagonal Laves phases Na_2K and K_2Cs as a function of the structural parameters c/a (axial ratio), z and x (cf. Table I). Varying z shifts the position of the larger A atoms in the direction of the z axis: increasing z beyond its ideal value $\frac{1}{16}$ moves the A atoms within a ∇ or Δ layer away from the central plane built up by B atoms (the small open circles in Fig. 3), thereby the distance between A atoms belonging to adjacent layers is reduced. Correspondingly, reducing z approaches the A atom from both sides to the central B-atom plane. Varying x moves the B atoms parallel to the Kagomé-layer planes, distorting the tetrahedral arrangement of the B atoms.

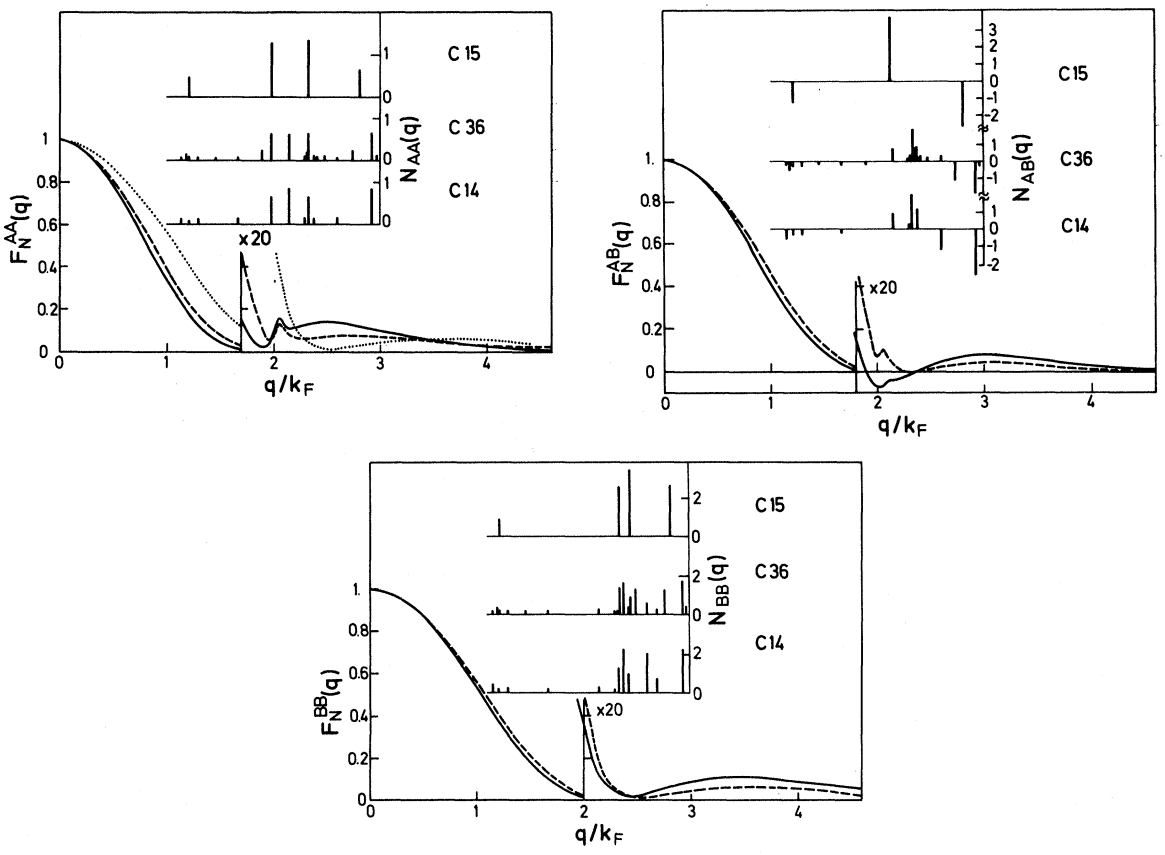

FIG. 4. Normalized energy-wave-number characteristics $F_N^{AA}(q)$ (a), $F_N^{AB}(q)$ (b), and F_N^{BB} (c) and the corresponding structural weight functions $N_{AA}(q)$, $N_{AB}(q)$, and $N_{BB}(q)$ for the three possible Laves-phase structures of the compounds Na_2K (full lines) and K_2Cs (broken lines). In (a) we included also the characteristic for K-K majority atom interactions in K_2Cs to allow for comparison with the K-K minority interactions in Na_2K (dotted line).

As we have already seen (cf. Table I), the electrostatic energy of a binary array of point ions of equal valence ($Z_A = Z_B$) has its minimum (as a function of the structural parameters at constant atomic volume) for a heavily distorted structure: $c/a = 1.52$, $x = -0.18$, $z = 0.070$. The effective valencies of the pure metals at their theoretical equilibrium volume are not very different: Na: $Z^* = 1.073$, K: $Z^* = 1.116$, and Cs: $Z^* = 1.162$. However, the effective valencies change on alloying, as has been pointed out in Sec. II. In the compound Na_2K, the effective valences of the components are now $Z^*_{Na} = 1.055$, $Z^*_K = 1.183$, and in K_2Cs $Z^*_K = 1.093$, $Z^*_{Cs} = 1.225$. In both cases the ratio of the effective valencies, which is about 1.04 for the pure metals, is enhanced to 1.12, the average Z^* remaining approximately constant. If the electrostatic energy is calculated using the actual effective valencies of Na_2K, we find a minimum at $c/a = 1.62$, $x = -0.175$, and $z = 0.0635$ (cf. top row of Fig. 5). The "charge transfer" related with the redistribution of the one orthogonalized-plane-wave charge density removes most of the anisotropy present in the Ewald energy of a lattice of ions with equal valencies. c/a and z are now very near their ideal values, hence the proper calculation of the effective valencies is sufficient to stabilize the wurtzite-like sublattice of the larger minority atoms.

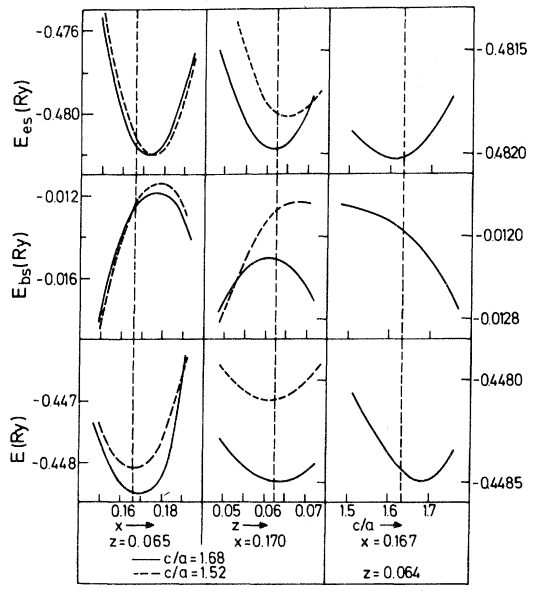

FIG. 5. Dependence of the electrostatic energy E_{es} (top row) of the band-structure energy E_{bs} (second row), and of the total energy (third row) of Na_2K on the axial ratio (third column) and on the structural parameters z and x (second and first columns) at the equilibrium volume. The first column refers to the left-hand energy scale, the other two to the right-hand scale.

The tetrahedral network of the majority atoms is still appreciably distorted. The band-structure contribution to the lattice energy displays a strong tendency towards anisotropy, quite analogously to the case of uniaxial pure metals (cf. the middle row of Fig. 5). However, if we combine E_{bs} with E_{es}, we see that the variation of the electrostatic energy with the structural parameters is dominant and that the effect of the band-structure energy is to remove the remaining distortions of the lattice, the calculated structural parameters being in very good agreement with experiment (cf. Table III). However, our theory predicts not only the crystal structure, but also the equilibrium lattice constants and the enthalpy of formation with a surprisingly high accuracy.

C. Phase stability

In Table II we have summarized the calculated equilibrium lattice constants, enthalpies, and volumes of formation. A negative enthalpy of formation is predicted for Na_2K, K_2Cs, and Rb_2Cs. The stability of the Laves phase has to be discussed in relation to the solid solution, taking into account the differences in the entropies of formation. Very little information is available on the last point. The entropy of formation of solid Na_2K at room temperature is quoted by Hultgren *et al.*[21] to be $\Delta S = -0.16$ cal/g atom K. No data are available for solid solutions. For liquid alkali-metal

TABLE III. Lattice constants, structural parameters, and enthalpies of formation for the Laves phases Na_2K and K_2Cs.

	Na_2K	
	theory	experiment
a (Å)	7.62	7.50 [a]
c (Å)	12.79	12.31 [a]
c/a	1.68	1.62
x	0.0635	0.0625
z	−0.1675	−0.1667
ΔH (cal/g atom)	−125	−145 [b]
	K_2Cs	
	theory	experiment
a (Å)	9.56	9.07 [c]
c (Å)	16.26	14.76 [c]
c/a	1.70	1.63
x	0.064	0.0625
z	−0.167	−0.1667
ΔH (cal/g atom)	−180	< 0

[a] Reference 5, room temperature.
[b] Reference 21, $T = 280$ °K.
[c] Reference 2, $T = 178$ °K.
[d] Reference 2, $T = 223$ °K.

alloys, the entropy of formation is given to 90% by the ideal mixing term. If we assume that this does not appreciably change in the solid, we can estimate the entropy of formation for the solid alloy to be $\Delta S = 1.3$ cal./g. atom K. ΔH is large and positive for a Na_2K solid solution, hence the ordered compound is stable up to the melting point. In order to be able to give a rough estimate of the temperature range of stability for the ordered compound, we assume ΔH and ΔS to be independent of temperature and calculate the transition temperature using $T_C = (\Delta H_{\text{sol sol}} - \Delta H_{\text{Laves}})/(\Delta S_{\text{sol sol}} - \Delta S_{\text{Laves}})$, where we take $\Delta S_{\text{sol sol}}$ to be that of an ideal solution and $\Delta S_{\text{Laves}} = \Delta S_{Na_2K}$. Using our calculated enthalpy of mixing, we obtain $T_C = 612$ °K (K_2Cs), $T_C = 174$ °K (Rb_2Cs), using the empirical estimates of ΔH,[22] we have $T_C = 240$ °K (K_2Cs), $T_C = 98$ °K (Rb_2Cs), experimentally $T_C \approx 180$ °K (K_2Cs).[3] The important thing is not a numerical agreement with experiment (which we can hardly expect to be quantitative), but the correct trend: Rb_2Cs is predicted to be stable only at temperatures which are much lower than the formation temperature of K_2Cs. Experimentally, Rb-Cs alloys have been investigated down to + 90 °K, no indications for compound formation have been found in that range. Compared to the random solid solutions, the calculated excess volumes of formation are more negative for systems with large differences in the atomic size of the component. This reflects the fact that different atoms may be stored more easily in a Laves than in a bcc lattice. For K-Rb and Rb-Cs the situation is reversed: the atoms have nearly equal size and the bcc solid solution has the higher density. The calculated isothermal bulk moduli of the compounds are nearly identical with those of the solid solutions (cf. Fig. 2a). For Na_2K and K_2Cs, the bulk modulus is smaller than given by the rule of mixture. This emphasizes the pure-metallic character of the compound.

Our theory fails to explain the existence of the Laves phase Na_2Cs. We calculate large positive enthalpies of formation for both Na_2Rb and Na_2Cs, which are not appreciably reduced by varying the structural parameters. It is well known that under moderately high pressure Cs behaves as a transition metal.[30] Covalent bonding charge is built up along the lines joining nearest neighbors. Of course it is impossible to describe such a situation within our model of overlapping spherical "pseudoatom" charge distributions. The situation is not very different if we increase the electronic charge density around a Cs ion by compressing the pure metal or by introducing it in a matrix of Na host ions with a much higher electron density. In this connection we refer to the large negative excess volume of Na_2Cs (Table V). A further hint to the important role of $s-d$ hybridization is the nonexistence of the compound Na_2Rb, whereas in the alkaline-earth systems all the corresponding hexagonal Laves phases Mg_2Ca, Mg_2Sr, and Mg_2Ba exist. Hence Cs should be treated as a transition metal in the compound Na_2Cs.

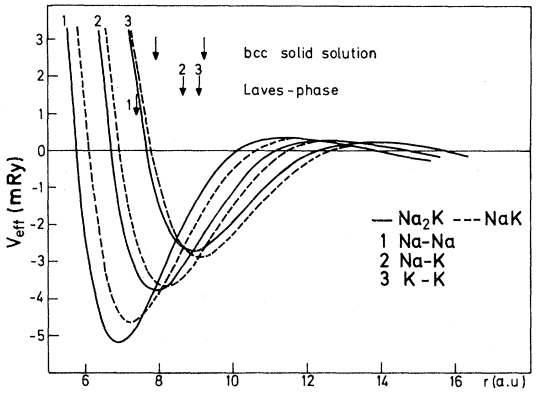

FIG. 6. Effective interionic pair potentials for Na_2K and NaK (solid and broken lines, respectively) at the equilibrium volume. The arrows indicate the nearest-neighbor distances in the $C14$ and in the bcc structures.

D. Interatomic forces

It is interesting to discuss the stability of the Laves phases in terms of the effective interionic pair potentials introduced in Sec. III. Figures 6 and 7 demonstrate that for the compound-forming systems Na_2K and K_2Cs the minima in the interionic potentials correspond very well to the nearest neighbor distances in the Laves phase structure. The effective pair potential is built up by two largely compensating contributions, the repulsive Coulomb and the attractive interaction via the valence electrons. Thus the pair poten-

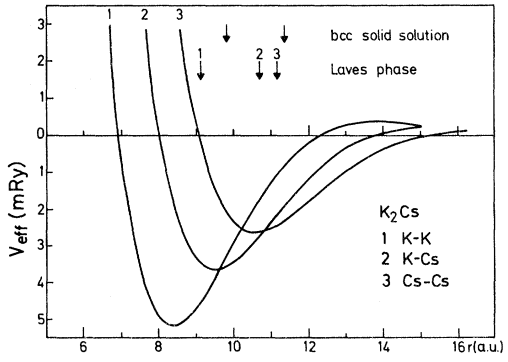

FIG. 7. Effective interionic pair potentials for K_2Cs (cf. Fig. 6).

tials illustrate the fact that the structure of the Laves phase is determined by the principle of close packing, which is realized by a delicate balance between electrostatic and electronic forces. The shape of the pair potentials explains why a bcc solid solution is energetically less favorable in these cases.

VII. INTERMETALLIC COMPOUNDS WITH A_6B_7 STOICHIOMETRY

An alternative sandwich of layers is built up of a central hexagonal layer of A atoms, two triangular layers of A atoms (centering the hexagons), and two Kagomé nets of B atoms (the triangles over the central A atoms) in centrosymmetric positions.[1] The usual shorthand notation for directly superposed Kagomé nets with this type of in-filling is O. The repeated sequence of O layers defines the Al_3Zr_4 structure[31] to be discussed in Sec. VIII. Using again ∇ and Δ to describe the Laves-type Kagomé stacking (with the corresponding in-filling between them), any sequence of O, ∇, and Δ defines a conceivable structure.[1] Repeated ∇O layers make the μ phase ($D8_5$, typified by Fe_7W_6 and Co_7Mo_6).[32] Repeated $\nabla O\Delta O$ layers built the structure of K_7Cs_6.[3] A further combination yielding a compound with A_6B_7 stoichiometry is $\nabla\Delta OO$, one the hypothetical structures explicitely mentioned by Frank and Kasper.[1] Table IV summarizes the crystallographic information and the Ewald coefficients, the positional parameters being given for the observed and the ideal structures of the μ phase and of K_7Cs_6. The ideal parameters are obtained by assuming ideal in-filling of the O and Δ,∇ layers and using $d=a$ and $d=\frac{1}{2}(\frac{8}{3})^{1/2}a$ for the distances between the Kagomé-nets in the O and in the ∇,Δ layers. The parameters for the hypothetical A_6B_7 structure are calculated in the same way. In Fig. 8, the three

TABLE IV. Crystallographic description and Ewald coefficients for the Frank-Kasper phases with A_6B_7 stoichiometry. The structural parameters are given for the ideal structures, with the observed parameters in parentheses. The Ewald coefficients are given also for the parameters minimizing the electrostatic energy for $Z_A=Z_B$. $\alpha=\alpha_{AA}+\alpha_{AB}+\alpha_{BB}$.

$D8_5$—Co_7Mo_6 type		Space group $R\bar{3}-D_{3h}^5$		
Atomic positions (in a hexagonal unit cell):				
6 Mo(1) atoms in (c), $z=\frac{1}{6}$ (0.1655); 6 Mo(2) in (c), $z=0.3526$ (0.3483);				
6 Mo(3) in (c), $z=0.4552$ (0.4518); 3 Co(1) in (a); 16 Co(2) in (h),				
$x=\frac{1}{6}$ ($\frac{1}{6}$), $z=-0.2562$ (−0.2584).				
Axial ratio: $c/a=5.45$ (5.38)				
Ewald coefficients:	α_{AA}	α_{AB}	α_{BB}	α
Ideal structure	−0.544 175	−0.647 638	−0.578 190	−1.770 002
Observed structure	−0.557 958	−0.611 739	−0.602 004	−1.771 701
z [Mo(2)] = 0.350				
z [Mo(3)] = 0.458	−0.544 649	−0.616 476	−0.614 297	−1.775 422
$c/a=5.3$				
K_7Cs_6 type		Space group $P6_3/mmc-D_{6h}^4$		
Atomic positions:				
2 Cs(1) atoms in (b); 2 Cs(2) in (c); 4 Cs(3) in (f), $z=0.97125$ (0.9769);				
4 Cs(4) in (f), $z=0.8175$ (0.8208); 2 K(1) in (a); 12 K(2) in (k),				
$x=\frac{1}{6}$ ($\frac{1}{6}$), $z=0.1124$ (0.1150).				
Axial ratio: $c/a=3.633$ (3.629).				
Ewald coefficients:	α_{AA}	α_{AB}	α_{BB}	α
Ideal structure	−0.547 710	−0.637 783	−0.584 698	−1.770 190
Observed structure	−0.553 746	−0.623 254	−0.594 748	−1.771 749
z (Cs3) = 0.974				
z (Cs4) = 0.810	−0.529 568	−0.651 135	−0.594 748	−1.775 451
$c/a=3.63$				
Hypothetical A_6B_7 type		Space group $P\bar{6}m2-D_{3h}^1$		
Atomic positions:				
2 $A(1)$ atoms in (g), $z=0.1376$; 2 $A(2)$ in (h), $z=0.1376$; 2 $A(3)$ in (h),				
$z=0.4156$; 2 $A(4)$ in (i), $z=0.0688$; 2 $A(5)$ in (i), $z=0.2064$; 2 $A(6)$ in (i),				
$z=0.3595$; 2 $B(1)$ in (g), $z=0.3875$; 6 $B(2)$ in (n), $x=\frac{1}{6}$, $z=0.2572$;				
3 $B(3)$ in (j), $x=\frac{1}{6}$; 3 $B(4)$ in (k), $x=\frac{1}{6}$.				
Axial ratio: $c/a=3.633$				
Ewald coefficients:	α_{AA}	α_{AB}	α_{BB}	α
Ideal structure	−0.465 158	−0.827 637	−0.471 634	−1.764 429

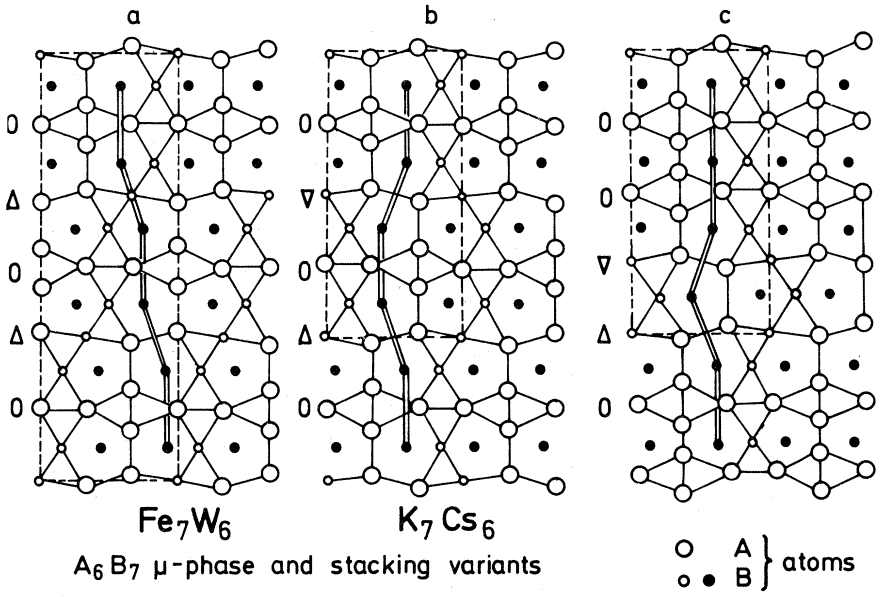

FIG. 8. Comparison of the three A_6B_7 lattices in form of a projection into the (110) plane (cf. Fig. 5).

structures are compared in form of a projection into the (110) plane. As for the Laves phases, the atoms of the secondary layers (full dots) center the pentagons of the primary layers (open circles). As a consequence, the secondary networks are now constructed of rectangles (in the O-regions) and triangles (in the ∇,Δ regions). This representation underlines the relationship between the K_7Cs_6 and the μ-phase structures, which is analogous to that between the hexagonal and cubic Laves phases.

A. Crystal structure of K_7Cs_6 and of similar compounds

One of the prominent features of the μ phase and of its stacking variants are the close distances between the large minority atoms in the O-like regions of the lattice, which are of the same magnitude than those between the small majority atoms. In the observed structures, these distances are enhanced by 2.9% (K_7Cs_6) and 5.1% (Co_7Mo_6), respectively, against the ideal lattice. These close interatomic distances are quite easily understood in a transition-metal compound, but in the K_7Cs_6 lattice, the shortest Cs-Cs distances are considerably smaller than in pure Cs. Hence it is interesting to calculate the binding energy at least as a function of those structural parameters which influence these distances. These parameters are the z values for the Mo(2) and Mo(3) atoms and for the Cs(3) and Cs(4) atoms, respectively. For the remaining structural parameters, the observed values are used. Varying the z's means to shift the four large atoms lying on a straight line in Fig. 8(a) and 8(b) against each other. In Table IV we have summarized the calculated Ewald coefficients for the ideal and the observed parameters and for those parameters minimizing the Ewald energy for $Z_A = Z_B$. Again the electrostatic energy for $Z_A = Z_B$ prefers a quite strongly distorted lattice: the short interatomic distances are shrinked with respect to the ideal structure, the Cs(4)-Cs(4) distances in the K_7Cs_6-structure by 12.8%, the distance between Cs atoms in Mo(3)-sites by 8.4%, assuming the Co_7Mo_6 structure. With respect to the observed structures, the corresponding figures are 15.3, respectively 12.9%. The above-mentioned "charge-transfer" effect (the effective valencies in K_7Cs_6 at the equilibrium volume are $Z^*_{Cs} = 1.213$, $Z^*_K = 1.088$) removes most of the distortion, the parameters of the energetically most favorable structure are now $z[\mathrm{Cs}(3)] = 0.976$, $z[\mathrm{Cs}(4)] = 0.815$, $c/a = 3.63$ in the K_7Cs_6 structure, and $z[\mathrm{Mo}(2)] = 0.348$, $z[\mathrm{Mo}(3)] = 0.457$, $c/a = 5.40$ for K_7Cs_6, assuming the Co_7Mo_6 structure. If the band-structure contributions are added, we obtain the equilibrium values for the lattice constants, structural parameters, and enthalpies of formation listed in Table V for K_7Rb_6, K_7Cs_6, and Rb_7Cs_6 with K_7Cs_6-type structure and for K_7Cs_6 and Rb_7Cs_6, assuming the μ-phase structure. For the remaining possible A_6B_7 phases, the enthalpy of formation is calculated only for the observed structural parameters (cf. Table IV) and compiled in Table VI. The K_7Cs_6 structure is the energetically most favorable in each case. Using the observed structural parameters, we obtain a negative enthalpy of formation only for Rb_7Cs_6. However, the enthalpy is quite sensitive against small variations of the structural parameters. The calculated

TABLE V. Equilibrium lattice constants, structural parameters, and enthalpies of formation for K_7Cs_6- and Co_7Mo_6- type intermetallic compounds.

	K_7Cs_6	
	theory	experiment [a]
a (Å)	9.68	9.08
c (Å)	37.29	32.95
c/a	3.85	3.629
z [Cs(3)]	0.975	0.9769
z [Cs(4)]	0.825	0.8208
ΔH (cal/g atom)	−65	<0

Compound structure	K_7Rb_6 K_7Cs_6	K_7Cs_6 Co_7Mo_6	Rb_7Cs_6 K_7Cs_6	Rb_7Cs_6 Co_7Mo_6
a (Å)	9.25	9.64	10.08	10.01
c (Å)	35.14	56.86	38.51	59.07
c/a	3.80	5.9	3.82	5.9
z [Cs(3), Mo(2)]	0.973	0.351	0.973	0.350
z [Cs(4), Mo(3)]	0.822	0.450	0.825	0.450
ΔH (cal/g atom)	−15	220	−120	20

[a] Reference 3.

structural parameters for the K_7Cs_6-type phases agree quite well (within 5%) with the measured parameters of K_7Cs_6.[3] The remaining differences in the z parameters act in such a way that the shortest Cs-Cs distances [Cs(4)-Cs(4)] are enhanced by 5.9% with respect to the observed arrangement, at the cost of the Cs(3)-Cs(4) distances which are reduced by 2.6%. The distances Cs(4)-Cs(4) and Cs(3)-Cs(4) (these ions lie on a straight line in z direction, cf. Fig. 8) are now almost identical. Furthermore, the axial ratio is enhanced by 6%. The same applies—mutatis mutandis—to the calculated μ-phase structure. Remembering that the purely electrostatic interactions prefer Cs-Cs distances which are 15% smaller than the observed ones, we see that the actual structure of K_7Cs_6 is the result of a delicate balance between electrostatic and electronic terms. In view of the complex nature of the compound, the achieved accuracy is certainly very encouraging.

The calculated excess volumina of formation (Table VII) are connected with the enthalpies of formation in the same way as for the Laves phases and for the solid solutions: a nearly vanishing volume of formation is related to the lowest enthalpy of formation. The bulk moduli of the intermetallic compounds again practically coincide with those of the corresponding solid solutions.

B. Phase stability and interatomic forces

Our theory predicts a negative enthalpy of formation for K_7Rb_6, K_7Cs_6, and Rb_7Cs_6. Experimentally only K_7Cs_6 is known to exist at temperatures below 178°K. Again the stability of the compounds has to be discussed in relation to the competing solid solutions and Laves phases. If we estimate the temperature for the compound—solid solution transition temperature in the same manner as for the Laves phases (assuming the same estimate for the entropy of formation) we find that the transition temperature for K_7Rb_6 should be lower by a factor of 4, that of Rb_7Cs_6 by a factor of 1.5 to 2 than that of K_7Cs_6. Hence our theory predicts stable phases of K_7Rb_6 and Rb_7Cs_6 only at very low temperatures. No experimental investigations have been made in that temperature range.

Again it is instructive to throw a rapid look on the effective interionic pair potentials (Fig. 9). According to the large number of crystallographically inequivalent sites and to the deviation from the ideal structure, the nearest neighbor distances are now split of, but they fit quite well into the minima of the pair potentials.

VIII. Al_3Zr_4-TYPE COMPOUNDS

The K_7Cs_6-type compounds are composed of regions which are isostructural to the Laves phases—and indeed the phase K_2Cs exists—and regions which are isostructural to the Al_3Zr_4 structure. Hence it is interesting to investigate

TABLE VI. Enthalpy (in cal/g atom) and excess volume (in percent) of formation for binary alkali compounds with A_6B_7 stoichiometry (calculated using the observed structural parameters).

	Structure	Na_7K_6	Na_7Rb_6	Na_7Cs_6	K_7Rb_6	K_7Cs_6	Rb_7Cs_6
ΔH	K_7Cs_6	845	1870	3430	41	150	−120
	Co_7Mo_6	1090	2150	3940	230	466	130
	A_6B_7	1660	2411	3600	260	350	75
$\Delta\Omega/\Omega$	K_7Cs_6	−2.1	−3.6	−9.0	2.5	−0.8	−0.2
	Co_7Mo_6	−1.9	−3.0	−8.1	2.7	−0.1	0.5
	A_6B_7	−1.7	−3.1	−9.9	2.9	−1.5	−0.2

TABLE VII. Crystallographic description and Ewald coefficients for the Al_3Zr_4 structure (see Table I for notation).

Al_3Zr_4 type		Space group $P\bar{6}-C_{3h}^1$		
Atomic positions:				
3 Al atoms in (j), $x=\frac{1}{3}$, $y=\frac{1}{6}$;				
2 Zr(1) atoms in (h), $z=\frac{1}{4}$; 1 Zr(2) in (f); 1 Zr(3) in (b).				
Axial ratio: $c/a=1$				
Ewald coefficients:				
Ideal structure	−0.449 350	−0.544 329	−0.777 983	−1.771 662
$z=0.275$ $c/a=0.975$	−0.457 412	−0.554 828	−0.765 164	−1.777 404

whether the latter structure (made up by repeated O-stacking) can exist in binary alkali metal systems. In Table VII we summarize the crystallographic information and the Ewald-coefficients for the Al_3Zr_4 lattice. There is an appreciable difference between the ideal and the electrostatically most favorable structure: quite analogously to the K_7Cs_6 structure, the electrostatic energy prefers Zr(1) atoms (they correspond to the Cs(4) atoms) which are closer together than in the ideal structure. Taking the orthogonalization holes into account (via the effective valences), the structural parameters are modified to $z=0.273$ and $c/a=0.975$, a full calculation yields $z=0.240$ and $c/a=0.98$ for K_3Cs_4 at the zero-pressure volume. Again the high symmetry of the ideal structure is stabilized only by the interplay of ionic and electronic forces. The enthalpy of formation is always positive: K_3Rb_4: $\Delta H=200$ cal./g. atom, K_3Cs_4: $\Delta H=600$ cal/g. atom, and Rb_3Cs_4: $\Delta H=90$ cal/g. atom. No intermetallic compound with this stoichiometry is predicted to exist in the alkali-metal systems.

IX. CONCLUSIONS

We have presented a first-principles calculation of the crystal structure, the equilibrium lattice constants and the enthalpy of formation for random alloys and for different ordered intermetallic compounds between alkali metals. For the disordered alloys, our calculation predicts an ideal-solution behavior, the enthalpies of mixing obeying a Hume-Rothery 15% rule if plotted against the ratio of the atomic radii of the components.

The crystal structures of the intermetallic compounds are described with very good accuracy in terms of a delicate balance between electrostatic and electronic terms. The redistribution of the valence-electron density due to orthogonalization effects (taken into account via the appropriately calculated concentration- and volume-dependent effective valences) plays an important role in determining the crystal structure. The interplay between Coulomb and band-structure forces is also demonstrated by the shape of the interionic pair potentials in relation to the interionic distances in the compounds.

The calculated enthalpies of formation are—as far as comparison with experimental data is possible—of surprisingly good accuracy. The theory

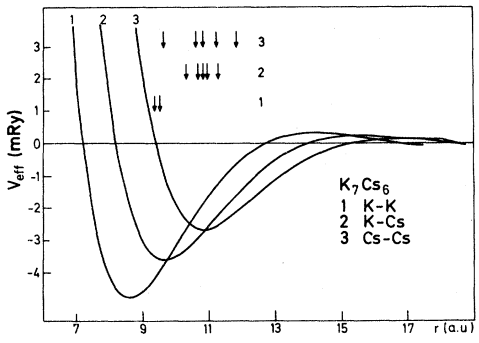

FIG. 9. Effective interionic pair potentials in K_7Cs_6. The arrows indicate interatomic distances occuring in the observed K_7Cs_6 structure.

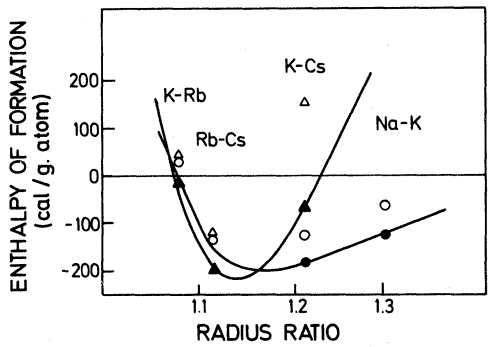

FIG. 10. Enthalpies of formation of intermetallic compounds against the ratio of the atomic radii of the components. Δ Laves phase $C14$ (ideal structural parameters), ▲ Laves phase $C14$ (calculated structural parameters), ○ K_7Cs_6 structure (observed structural parameters), ● K_7Cs_6 structure (calculated structural parameters).

verifies successfully the existence of the compounds Na_2K (up to the melting point) and K_2Cs and K_7Cs_6 (at lower temperatures only). The possible existence of similar intermetallic phases in the Rb-Cs system is predicted at very low temperature (below 90 °K). In this region, compound formation is possibly hindered by the low mobility. Our theory fails to describe the Laves phase Na_2Cs. Evidence is given that Cs should be treated as a transition metal in this phase.

The physical principle governing compound formation is shown to be close packing. This is illustrated in Fig. 10, where we have plotted the enthalpies of formation against the radius ratio. Here we have to remember that our calculation is entirely from first-principles and that, for the reason outlined above, our calculated radius ratio is slightly different from the observed one. In fact, the enthalpy of formation K_7Cs_6 is slightly too low compared to that of K_2Cs. At the observed radius ratio of K-Cs however, the conditions for the coexistence of both phases are optimally fulfilled.

The principle of close-packing should not be interpreted in terms of hard spheres, but more physically in terms of the soft interionic pair potentials presented here. An intermetallic phase is formed when the interatomic distances given by its structure are compatible with the minima of the pair potentials.

The interionic potentials in the alloy are quite different from those in the pure metals. The success of our calculation underlines the usefulness of the concept of pseudopotential optimization for describing even highly complex intermetallic phases of simple metals.

ACKNOWLEDGMENTS

The author would like to thank Professor H. Bilz for his continuous support and encouragement, Professor A. Simon for many stimulating discussions, and Professor E. O. Kane for a critical reading of the manuscript.

[1]F. C. Frank and J. S. Kasper, Acta Crystallogr. 11, 184 (1958); 12, 483 (1959).
[2]A. Simon and G. Ebbinghaus, Z. Naturforsch. B29, 618 (1974).
[3]A. Simon, W. Brämer, B. Hillenköter, and H. J. Kullman, Z. Anorg. Allg. Chem. 419, 253 (1976).
[4]Struct. Rep., the continuation of the *Strukturbericht*, published for the International Union for Crystallography (N.V.A. Oosthoek's Uitgevers MIJ, Utrecht, Netherlands).
[5]F. Laves and H. J. Wallbaum, Z. Anorg. Chem. 250, 110 (1942).
[6]E. Rinck, Compt. Rend. 199, 1217 (1934).
[7]C. Goria, Gazz. Chim. Ital. 65, 1226 (1935).
[8]W. A. Harrison, *Pseudopotentials in the Theory of Metals* (Benjamin, New York, 1966).
[9]J. Hafner, J. Phys. F 6, 1243 (1976).
[10]J. Hafner, in Proceedings of the Third International Conference on Liquid Metals, Bristol, 1976, edited by R. Evans and D. Greenwood (The Institute of Physics, London, to be published).
[11]We use atomic units in the pseudopotential calculations. The final results, however are converted to the more usual units of cal/g atom for enthalpies and Å for lattice dimensions.
[12]J. C. Phillips and L. Kleinman, Phys. Rev. 116, 287 (1959).
[13]M. H. Cohen and V. Heine, Phys. Rev. 122, 1821 (1961).
[14]P. Vashishta and K. S. Singwi, Phys. Rev. B 6, 875 (1972).
[15]J. Hafner, Z. Phys. B 22, 351 (1975).
[16]J. Hafner, Z. Phys. B 24, 41 (1976).
[17]K. Fuchs, Proc. R. Soc. A 151, 585 (1935).
[18]G. L. Krasko, Sov. Phys.-JETP Lett. 13, 155 (1971).
[19]T. M. Hayes, H. Brooks, and A. Bienenstock, Phys. Rev. 175, 699 (1968).
[20]J. E. Inglesfield, J. Phys. C 2, 1285 (1969).
[21]R. Hultgren, R. L. Orr, P. D. Anderson, and K. K. Kelley, *Selected Values of Thermodynamic Properties of Metals and Alloys* (Wiley, New York, 1963).
[22]T. Yokokawa and O. J. Kleppa, J. Chem. Phys. 40, 46 (1964).
[23]*International Tables for X-Ray Crystallography*, edited by N. F. Henry and K. Lonsdale (Kynoch, Birmingham, 1969), Vol. I.
[24]J. H. Wernick, in *Intermetallic Compounds*, edited by J. H. Westbrook (Wiley, New York, 1967), p. 197.
[25]M. Hansen and K. Anderko, Constitution of Binary Alloys (McGraw-Hill, New York, 1958).
[26]J. Hafner, Phys. Rev. B 10, 4151 (1974).
[27]M. B. McNeil, J. Phys. C 3, 2020 (1970).
[28]W. Hoinka, G. Müller, and H. Woittenek, Wiss. Z. Tech. Univ. Dres. 21, 493 (1972).
[29]R. Hoppe (unpublished).
[30]S. G. Louie and M. L. Cohen, Phys. Rev. B 10, 3237 (1974).
[31]C. G. Wilson, D. K. Thomas, and F. J. Spooner, Acta Crystallogr. 13, 56 (1960).
[32]J. B. Forsyth and L. M. d'Alte da Veiga, Acta Crystallogr. 15, 543 (1962).